

Photodisintegration of Ultrahigh Energy Cosmic Rays: A New Determination

F. W. Stecker

Laboratory for High Energy Astrophysics, Code 661,
NASA/Goddard Space Flight Center, Greenbelt, MD 20771, USA.

M. H. Salamon

Physics Department, University of Utah, Salt Lake City, UT 84112

ABSTRACT

We present the results of a new calculation of the photodisintegration of ultrahigh energy cosmic-ray (UHCR) nuclei in intergalactic space. The critical interactions for energy loss and photodisintegration of UHCR nuclei occur with photons of the 2.73 K cosmic background radiation (CBR) and with photons of the infrared background radiation (IBR). We have reexamined this problem making use of a new determination of the IBR based on empirical data, primarily from IRAS galaxies, consistent with direct measurements and upper limits from TeV γ -ray observations. We have also improved the calculation by including the specific threshold energies for the various photodisintegration interactions in our Monte Carlo calculation. With the new smaller IBR flux, the steepness of the Wien side of the now relatively more important CBR makes their inclusion essential for more accurate results. Our results indicate a significant increase in the propagation time of UHCR nuclei of a given energy over previous results. We discuss the possible significance of this for UHCR origin theory.

Subject headings: cosmic rays, background radiations

1. Introduction

Shortly after the discovery of the cosmic microwave background radiation (CBR), it was shown that cosmic ray protons above ~ 60 EeV (6×10^{19} eV) should be attenuated by photomeson interactions with CBR photons (Greisen 1966, Zatsepin & Kuzmin 1966, Stecker 1968). It was later calculated that heavier cosmic ray nuclei with similar

total energies would also be attenuated, but by a different process, *viz.*, photodisintegration interactions with IBR photons (Puget, Stecker & Bredekamp 1976), hereafter designated PSB). We will refer to such cosmic rays of total energies above 10 EeV as ultrahigh energy cosmic rays (UHCR).

In the more conventional scenario, UHCRs are charged particles which must be accelerated to ultrahigh energies by electromagnetic processes at extragalactic sites, both because there are no known sites in our galaxy which can accelerate and magnetically contain them and also because most of the observed UHCR air shower events arrive from directions outside of the galactic plane. Although such acceleration of charged particles to energies above 100 EeV in cosmic sources pushes our present theoretical ideas to their extreme, it has been suggested that it may occur in hot spots in the lobes of radio galaxies (Biermann & Strittmatter 1987, Takahara 1990).

The detection of the two highest energy air shower events yet observed, with energies of ~ 200 (between 170 and 260) EeV (Hayashida *et al.* 1994) and 320 ± 90 EeV (Bird *et al.* 1995) has aggravated both the acceleration and propagation problems for cosmic-ray physicists. (Very recently, the AGASA group has presented a total of 6 events of energies between ~ 100 and ~ 200 EeV, including the one cited above, observed since 1990 (Takeda *et al.* 1998).) How does nature accelerate particles to these extreme energies and how do they get here from extragalactic sources (Elbert & Sommers 1995)? To answer these questions, new physics has been invoked, physics involving the formation and annihilation of topological defects (TDs) which may have been produced in the very earliest stages of the big bang, perhaps as a result of grand unification. A TD annihilation or decay scenario has unique observational consequences, such as the copious production of UHCR neutrinos and γ -rays (Sigl 1996 and refs. therein; Bhattacharjee, Shafi, & Stecker 1998). A new ground-based detector array experiment named after Pierre Auger (Cronin 1992) and an interesting satellite experiment called *OWL* (Ormes *et al.* 1997) have been proposed to test look for such consequences.

2. Propagation of UHCR Nuclei

A UHCR *proton* of energy ~ 200 EeV has a lifetime against photomeson losses of $\sim 3 \times 10^{15}$ s; one of energy 300 EeV has a lifetime of about half that Stecker (1968). These values correspond to linear propagation distances of ~ 30 and 15 Mpc respectively. Even shorter lifetimes were calculated for Fe nuclei, based on photodisintegration off the IBR (PSB). Recent estimates of the lifetimes of UHCR γ -rays against electron-positron pair production interactions with background radio photons give values below 10^{15} s (Protheroe

& Biermann 1996). Within such distances, it is difficult to find candidate sources for UHCRs of such energies.

In this paper, we reexamine a part of the propagation problem by presenting the results of a new calculation of the photodisintegration of UHCR *nuclei* through the CBR and IBR in intergalactic space. In order to do this, we have made use of a new determination of the IBR based on empirical data, primarily from IRAS galaxies, recently calculated by Malkan & Stecker (1998).¹

They calculated the intensity and spectral energy distribution (SED) of the IBR based on empirical data, some of which was obtained for almost 3000 IRAS galaxies. It is these sources which produce the IBR. The data used for the new IBR calculation included (1) the luminosity dependent SEDs of these galaxies, (2) the 60 μm luminosity function for these galaxies, and (3) the redshift distribution of these galaxies. The magnitude of the IBR flux derived by Malkan & Stecker (1998) is considerably lower than that used in PSB in their extensive examination of the photodisintegration of UHCR nuclei.

A search for absorption in the high energy γ -ray spectra of extragalactic sources can also be used to help determine the value of the IBR or to place constraints on the magnitude of its flux (Stecker, De Jager, & Salamon 1992). The observed lack of strong absorption in the γ -ray spectra of the active galaxies Mrk 421 (McEnery *et al.* 1997) and Mrk 501 (Aharonian *et al.* 1997) up to an energy greater than $\sim 5\text{-}10$ TeV is consistent with the new, lower value for the IBR used here (Stecker & De Jager 1997, Stecker & De Jager 1998, Stanev & Franceschini 1998, Biller *et al.* 1998).

The SED calculated by Malkan & Stecker (1998) agrees with direct estimates of the far infrared background obtained from the *COBE/FIRAS* observations (Puget *et al.* 1996, Fixsen *et al.* 1997, Fixsen *et al.* 1998). Recent fluxes reported from *COBE/DIRBE* observations at 140 and 240 μm (Hauser *et al.* 1998) are roughly a factor of 2 higher than the Malkan & Stecker (1998) predictions, but are consistent with them if one considers the systematic uncertainties in the observational results (Dwek *et al.* 1998).

In justifying our reexamination of the photodisintegration problem using the new IBR

¹In a recent paper (Stecker 1998), one of us considered such photodisintegration interactions, using the new estimate of the extragalactic IR spectral energy distribution by (Malkan & Stecker 1998), which yielded an extragalactic IR photon density even lower than the LIR estimate used in PSB. That paper, however, neglected the fact that the lower IR flux used in the new calculation would imply that interactions with CBR photons would now be dominant above an energy of roughly 130 EeV, rather than 300 EeV (*cf.* Fig. 8 in PSB). Thus, as pointed out by Epele & Roulet (1998), it is important to include interactions with CBR photons in the calculation.

SED, we point out that it may reasonable to expect that the highest energy cosmic rays may be nuclei. This is because the maximum energy to which a particle can be accelerated in a source of a given size and magnetic field strength is proportional to its charge, Ze . That charge is 26 times larger for Fe than it is for protons. Although some composition measurements in the energy range 0.1-10 EeV appear to indicate a transition from heavier to lighter nuclei with increased energy (Gaisser *et al.* 1993), this and other data appear to be consistent with a “mixed” composition of both protons and heavier nuclei (Hayashida *et al.* 1995, Dawson, Meyhandan & Simpson 1998). In any case, at the “lower” energies for which composition measurements have been attempted, most of the cosmic rays may be galactic in origin.

3. Calculations

We have now done a full Monte Carlo calculation similar to that presented in PSB, but using the new intergalactic infrared spectrum given by Malkan & Stecker (1998). In this new calculation, we have also specifically included the threshold energies of the various nuclear species to photodisintegration. The reason that this is now important is that with the CBR playing a relatively more important role, interactions of the steeply falling cosmic-ray spectrum near threshold with the Wien tail of the CBR become important relative to the much flatter IBR photon spectrum. In fact, as we will show, taking account of the measured higher threshold energies (as opposed to the artificial value of 2 MeV taken by PSB) increases the value of the cutoff energy for heavy UHCR nuclei.

Our intent is to both update and improve the PSB results and also to determine if the highest energy CR events seen by the Fly’s Eye and Akeno groups are consistent with their being heavy nuclei that have propagated to us from candidate active galactic nuclei (Stecker 1998). The energy loss from photodisintegration has a much stronger dependence on Lorentz factor than on atomic weight, and increases strongly with Lorentz factor γ (PSB). Therefore, to maximize the propagation distance for a given total particle energy, $E = \gamma AM$ (where M is the nucleon mass), one takes the largest possible mass number. Given the abundances of the elements, this nucleus is Fe. Therefore (as PSB have done) we chose to examine the propagation history of ^{56}Fe only, as this nuclide offers the best chance for providing a conventional explanation for the UHCR events.

3.1. Cross Sections

The nuclear photodisintegration process is dominated by the giant dipole resonance (GDR), which peaks in the γ -ray energy range of 10 to 30 MeV (nuclear rest frame). Experimental data are generally consistent with a two-step process: photoabsorption by the nucleus to form a compound state, followed by a statistical decay process involving the emission of one or more nucleons from the nucleus (Levinger 1960). The photoabsorption cross section roughly obeys a Thomas-Reiche-Kuhn (TRK) sum rule, *viz.*,

$$\Sigma_d \equiv \int_0^\infty \sigma(\epsilon) d\epsilon = \frac{2\pi^2 e^2 \hbar N Z}{Mc A} = 60 \frac{NZ}{A} \text{mb-MeV}, \quad (1)$$

where A is the mass number, Z is the nuclear charge, $N = A - Z$, M is the nucleon mass and ϵ is the photon energy in the rest system of the nucleus. The TRK sum rule is not exact, however, owing to the presence of nuclear exchange forces (Feenberg 1936), as can be seen in Table 1 of PSB (which is based on the data tabulations of Fuller, Gerstenberg, Vander Molen, and Dunn (1973) and related material supplied by E. Fuller.)

PSB approximated the GDR cross section for a given nuclide (Z, A) with the parameterization

$$\sigma_i(\epsilon) = \begin{cases} \xi_i \Sigma_d W_i^{-1} e^{-2(\epsilon - \epsilon_{p,i})^2 / \Delta_i^2} \Theta_+(\epsilon_{\text{thr}}) \Theta_-(\epsilon_1), & \epsilon_{\text{thr}} \leq \epsilon \leq \epsilon_1, \quad i = 1, 2 \\ \zeta \Sigma_d \Theta_+(\epsilon_{\text{max}}) \Theta_-(\epsilon_1) / (\epsilon_{\text{max}} - \epsilon_1), & \epsilon_1 < \epsilon \leq \epsilon_{\text{max}} \\ 0, & \epsilon > \epsilon_{\text{max}} \end{cases} \quad (2)$$

where the Z and A dependence of the width Δ_i , the peak energy $\epsilon_{p,i}$, and the dimensionless integrated cross sections ξ_i and ζ are understood, and are listed in Table 1 of PSB. $\Theta_+(x)$ and $\Theta_-(x)$ are the Heaviside step functions, and the normalization constants W_i are given by

$$W_i = \Delta_i \sqrt{\frac{\pi}{8}} \left[\text{erf} \left(\frac{\epsilon_{\text{max}} - \epsilon_{p,i}}{\Delta_i / \sqrt{2}} \right) + \text{erf} \left(\frac{\epsilon_{p,i} - \epsilon_1}{\Delta_i / \sqrt{2}} \right) \right]. \quad (3)$$

The index i takes the values 1 or 2, corresponding to single or double nucleon emission during the photodisintegration reaction. For energies $\epsilon < \epsilon_1 = 30$ MeV, the measured cross sections are dominated by single $[(\gamma, n)$ or $(\gamma, p)]$ or double $[(\gamma, 2n), (\gamma, np), (\gamma, 2p)]$ nucleon loss, since the threshold energies for the emission of larger numbers of nucleons are close to or exceed ϵ_1 (Forkman & Petersson 1987). From ϵ_1 to $\epsilon_{\text{max}} = 150$ MeV, the cross section is approximated as flat, normalized so that the integrated cross section matches experimental values. The probability of emission of k nucleons in this region is given by a distribution function which is independent of the γ -ray energy (see Table 2 of PSB). Above ϵ_{max} , detailed cross section data are more scarce; we follow PSB by approximating this smaller residual cross section by zero. Interactions with photons of energy greater than ϵ_{max} will

have a negligible contribution to the photodisintegration process for UHCR energies below 1000 EeV owing to the fact that the density of the background photons seen by the UHCR near the peak of the GDR cross section falls rapidly with energy (exponentially along the Wien tail of the CBR, and roughly as ϵ^{-2} in IR-optical region), along with the fact that the photodissociation cross section is about two orders of magnitude lower in the γ -ray energy region from ϵ_{\max} to ~ 1 GeV than at the GDR peak (Jonsson & Lindgren 1973, Jonsson & Lindgren 1977). We have verified by numerical tests that interactions with photons of energy greater than ϵ_{\max} indeed have a negligible effect on our calculation.

In the PSB calculation, the GDR threshold energies were taken to be $\epsilon_{\text{thr}} = 2.0$ MeV for *all* reaction channels. This value is far smaller than the true thresholds; single-nucleon emission has a typical threshold of ~ 10 MeV, while the double-nucleon emission energy threshold is typically ~ 20 MeV. Table 1 lists the energy thresholds for the (γ, n) , (γ, p) , $(\gamma, 2n)$, (γ, np) , $(\gamma, 2p)$, and (γ, α) channels for each nuclide in the ^{56}Fe decay chain (taken from Forkman & Petersson, 1987). Owing to the increased importance of the CBR relative to the IBR that follows from the new, lower IBR estimates, and the presence of the Wien tail that exponentially increases the target photon density at the GDR threshold (see Figure 1), increasing this threshold energy may significantly lengthen the propagation distance of a highly relativistic nucleus. Therefore we have used the measured threshold energies for a subset of the reaction channels that are given in Table 1.

Unfortunately, photodisintegration cross section data are incomplete. For many reaction channels, $\sigma(\epsilon)$ data do not exist. Also, integrated cross section strengths are not available for all of the exclusive channels. The most complete compilation of the world's GDR cross section data exists in the 15 volumes of Fuller & Gerstenberg (1983). In these volumes GDR cross section data for ^{56}Fe , for example, are given only for the (γ, pX) channel and the inverse channels (α, γ) and (p, γ) .

One cannot perform the Monte Carlo calculations in such a way as to distinguish a (γ, n) interaction from a (γ, p) reaction when the relative branching ratios are not known. Instead, we separately consider only single-nucleon emission (as a single channel) and double-nucleon emission (as a single channel) in the GDR region up to ϵ_1 . We take the conservative approach of choosing the energy threshold for single-nucleon emission to be the *lowest* of the two for (γ, n) and (γ, p) for each nuclide in the decay chain, with a similar choice for the two-nucleon emission channel. Along most of the decay chain from ^{56}Fe to ^1H there is only one stable isotope for a given mass A . Since the radioactive decay time to the line of stability is less than the one-nucleon photodisintegration loss time for all but three unstable nuclei, ^{53}Mn , ^{26}Al , and ^{10}Be , we assume decay has brought the daughter nucleus to the line of stability before the next photon collision, so that for any given mass A there

is a unique charge Z . This clearly is not the case for mass values $A = 54, 50, 48, 46, 40$, and 36, where more than one stable isotope exists, but the absence of cross section data for each of these isotopes makes this a moot point.

We also note that although the thresholds are lowest for α emission (due to the α 's large binding energy), the integrated cross section for α emission from ^{56}Fe , for example, is over two orders of magnitude lower than the Σ_d value for that nuclide (Skopic, Asai, & Murphy, 1980; see also Fuller & Gerstenberg, 1983). We therefore neglect the α emission channels entirely in our calculation.

3.2. Reaction Rates

For a UHCR nucleus with Lorentz factor $\gamma = E/AM$ propagating through an isotropic soft photon background with differential number density $n(\epsilon)$, the photodisintegration rate R (lab frame) is given by (Stecker 1969)

$$R = \frac{1}{2} \int_0^\infty d\epsilon \frac{n(\epsilon)}{\gamma^2 \epsilon^2} \int_0^{2\gamma\epsilon} d\epsilon' \epsilon' \sigma(\epsilon'), \quad (4)$$

where σ is the total cross section, summed over the number of emitted nucleons.

In our calculations we construct the soft photon background by summing three components: (1) the $T = 2.73\text{K}$ cosmic background radiation (CBR) from lab frame energies of $\epsilon = 2.0 \times 10^{-6}$ eV to 4.0×10^{-3} eV, (2) the infrared background radiation (IBR) estimated by Malkan & Stecker (1998) from $\epsilon = 3.0 \times 10^{-3}$ eV to 0.33 eV (using the two “best estimates” shown by heavy lines in their Figure 2, which we denote as the “high IBR” and “low IBR” cases), and (3) the optical to UV diffuse, extragalactic photon background estimated by Salamon & Stecker (1998) (taking their no-metallicity-correction case) from $\epsilon = 0.33$ eV to 13 eV. Figure 1 shows the SED of the entire low energy background radiation. A salient feature of this figure is the roughly constant energy flux down to the dramatic rise of the Wien tail of the CBR. For UHCR nuclei with Lorentz factors large enough so that the CBR photons are above photodisintegration threshold, most of the reaction rate R is dominated by collisions with CBR photons. This is particularly true with the new, smaller IR photon background levels, compared to those used by PSB.

The energy loss time τ is defined as

$$\tau^{-1} \equiv \frac{1}{E} \frac{dE}{dt} = \frac{1}{\gamma} \frac{d\gamma}{dt} + \frac{R_1}{A} + \frac{2R_2}{A} + \frac{\langle \Delta A \rangle R_k}{A}, \quad (5)$$

where R_1 , R_2 , and R_k are the reaction rates for one- and two-nucleon emission, and R_k is the reaction rate for $\langle \Delta A \rangle > 2$ nucleon loss. The reduction in γ comes from two effects: nuclear

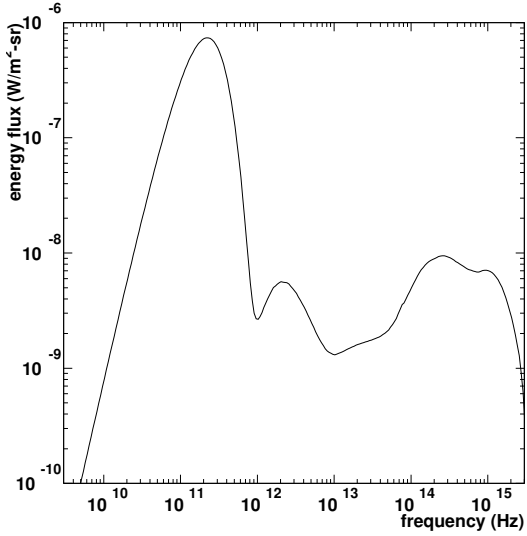


Fig. 1.— Energy flux spectrum (SED) of diffuse, intergalactic soft photon background.

energy loss due to electron-positron pair production off the CBR background, and the γ -ray momentum absorbed by the nucleus during the formation of the excited compound nuclear state that precedes nucleon emission. This latter effect is much smaller (of order $\sim 10^{-2}$) than the energy loss from nucleon emission and will therefore be neglected. For the former mechanism, we use the results given in Figure 3 of Blumenthal (1970), which gives the loss rate for relativistic nuclei off the CBR calculated in the first Born approximation. (We note that the Coulomb corrections to the Born approximation (Davies, Bethe & Maximon 1954, Jauch & Rohrlich 1980) have a negligible effect on the pair production loss rate for ultrarelativistic Fe nuclei.)

Figure 2 shows the energy loss rates due to single-nucleon, double-nucleon, and pair production processes for ^{56}Fe as a function of energy, along with the total energy loss rate. Also shown is the total energy loss rate when the photodisintegration thresholds ϵ_{thr} are all set to 2 MeV; this indicates the effect of incorporating more realistic threshold energies in the Monte Carlo calculation, compared to those of PSB.

3.3. Results

Figure 3 shows the spectra of ^{56}Fe nuclei after propagating linear distances from 1 to 1000 Mpc (corresponding to lifetimes between 10^{14} and 10^{17} s), assuming a source differential energy spectrum $\propto E^{-3}$ over the energy interval 10 to 1000 EeV. The effect of

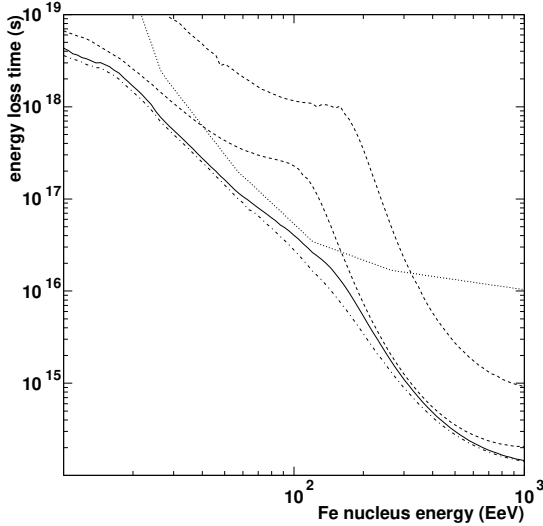


Fig. 2.— Energy loss times for single-nucleon (lower dashed line), double-nucleon (upper dashed line), and pair production processes (dotted line), and their total (solid line). The dash-dotted line shows the energy loss time using $E_{\text{thr}} = 2$ MeV for all photodisintegration rates, as was done in PSB.

the CBR “wall” at the Wien side of the 2.73K blackbody spectrum is to produce a sharp cutoff at a rather well defined energy, E_c .

Figure 4 shows the cutoff energy as a function of propagation time, where E_c is defined as the CR energy at which the propagated differential flux is $1/e$ that of the unpropagated flux. For comparison, the cutoff energies calculated by PSB are also shown. It can be seen that (except for energies above ~ 200 EeV) for a given energy, the propagation time increases by a substantial factor over that calculated by PSB, who assumed larger IBR fluxes and a 2 MeV threshold for all photodisintegration interactions. We also note that our new results do not differ significantly for the two SEDs adopted from Malkan & Stecker (1998) and, except for the longest propagation times, they do not differ significantly from the no-IBR case shown in the Figure. This is because the new values obtained for the IBR are so low.

4. Discussion and Conclusions

As can be seen from Figure 4, our use of the new, lower values for the intergalactic infrared photon flux, together with the explicit inclusion of the measured threshold energies

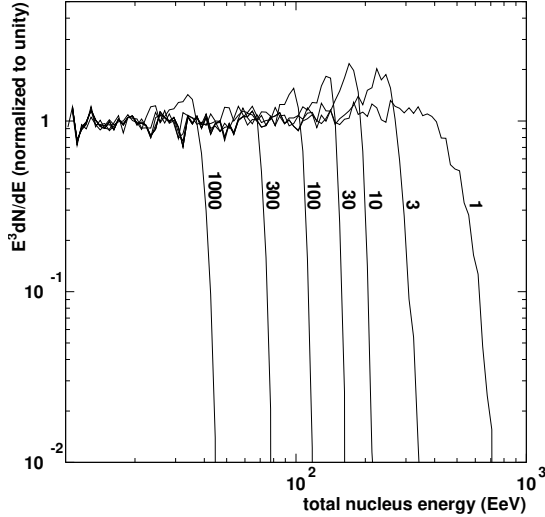


Fig. 3.— The differential spectra of ^{56}Fe after propagation over the distance (in Mpc) indicated for each curve. The initial, source spectrum is a power-law, E^{-3} , over the interval 10 to 1000 EeV.

for photodisintegration of the individual nuclides involved in the calculation, has the effect of increasing the cutoff energy (for a given propagation time) of heavy UHCR nuclei over that originally calculated by PSB. This increase may have significant consequences for understanding the origin of the highest energy cosmic ray air shower events.

Stanev, Biermann & Lloyd-Evans (1995) have examined the arrival directions of the highest energy events. They point out that the \sim 200 EeV event is within 10° of the direction of the strong radio galaxy NGC315. NGC315 lies at a distance of only ~ 60 Mpc from us. For that distance, our results indicate that heavy nuclei would have a cutoff energy of ~ 130 EeV, which may be within the uncertainty in the energy determination for this event. The \sim 300 EeV event is within 12° of the strong radio galaxy 3C134. The distance to 3C134 is unknown because its location behind a dense molecular cloud in our Galaxy obscures the spectral lines required for a redshift measurement. It may therefore be possible that *either* cosmic ray protons (Stecker 1968) *or* heavy nuclei originated in these sources and produced these highest energy air shower events.

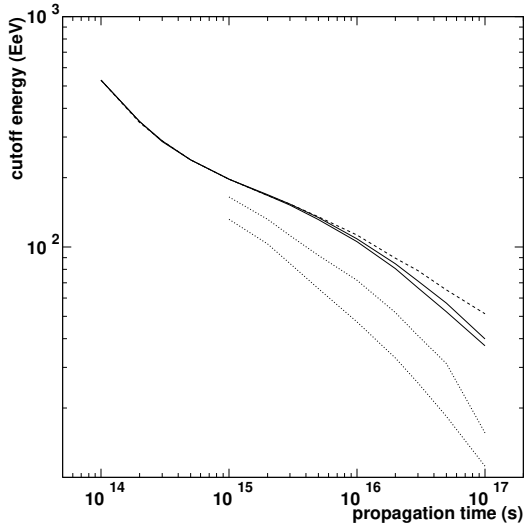


Fig. 4.— Cutoff energy versus propagation time for UHCR nuclei starting out as ^{56}Fe . The solid lines are for our new calculations using the two IBR SEDs from Malkan & Stecker (1998) and the higher threshold energies. The dashed line is calculated using only the CBR (no IBR). The dotted lines are the results from Fig. 16 of PSB and are shown for comparison. The lower the IBR, the higher the cutoff energy curve.

REFERENCES

- Aharonian, F. *et al.* 1997, Astron. & Ap 327, L5
- Bhattacharjee, P., Shafi, Q., & Stecker, F.W. 1998 Phys. Rev. Letters 80, 3698
- Biermann, P.L. & P.A. Strittmatter 1987, ApJ 322, 643
- Biller, S. *et al.* 1998, Phys. Rev. Letters 80, 2992
- Bird, D.G. *et al.* 1995, ApJ 441, 144
- Blumenthal, G.R., 1970, Phys. Rev. D1, 1596.
- Dwek, E. *et al.* 1998, e-print astro-ph/9806129
- Cronin, J.W. 1992, Nucl Phys. B (Proc. Suppl.) 28B, 213
- Davies, H., Bethe, H.A. & Maximon, L.C. 1954, Phys. Rev. 93, 788
- Dawson, B.R., R. Meyhandan & K.M. Simpson 1998 e-print astro-ph/9801260, submitted to Astropart. Phys.

- Elbert, J.W. & Sommers, P. 1995, ApJ 441, 151
- Epele L.N. & E. Roulet 1998, submitted to Phys. Rev. Letters
- Fixsen *et al.* 1997, ApJ 486, 623
- Fixsen *et al.* 1998, e-print astro-ph/9803021
- Feenberg, E., 1936, Phys. Rev. 49, 328
- Forkman, B. & Petersson, R., in *Handbook on Nuclear Activation Data* (1987), IAEA Tech. Rep. Series No. 273, 631
- Fuller, E.G. & Gerstenberg, H., 1983, U.S. National Bureau of Standards, Washington, D.C., Rep. NBSIR-83-2742.
- Fuller, E.G., Gerstenberg, H.M., Vander Molen, H., & Dunn, T.C., 1973, *Photonuclear Reaction Data, 1973*, NBS Special Publication 380.
- Gaisser, T. *et al.* 1993, Phys. Rev. D50, 5710
- Greisen, K. 1966, Phys. Rev. Letters 16, 748
- Hauser, M. *et al.* 1998, e-print astro-ph/9806167
- Hayashida, N. *et al.* 1994, Phys. Rev. Letters 73, 3491
- Hayashida, N. *et al.* 1995, J. Phys. G, 21, 1101
- Jauch, J.M. & Rohrlich, F. 1980, *The Theory of Photons and Electrons* (Springer-Verlag, Berlin)
- Jonsson, G.G. & Lindgren, K. 1973, Physica Scripta 7, 49
- Jonsson, G.G. & Lindgren, K. 1977, Physica Scripta 15, 308
- Levinger, J.S., *Nuclear Photodisintegration*, 1960 (Oxford:Oxford University Press)
- Malkan M.A. & F.W. Stecker 1998, ApJ 496, 13
- McEnery, J.E. *et al.* 1997, in Proc. 25th Intl. Cosmic Ray Conf. (Durban, S.A.) eds. M.S. Potgieter, *et al.* 3, 257
- Ormes, J.F. *et al.* 1997, in *Proc. 25th Intl. Cosmic Ray Conf.* (Durban, S.A.) eds. M.S. Potgieter, *et al.* 5, 273

- Protheroe, R.J. & P.L. Biermann 1996, Astroparticle Phys. 6, 45
- Puget, J.L., F .W. Stecker & J.H. Bredekamp 1976, ApJ 205, 638
- Puget *et al.* 1996, *A & A* 308, L5
- Salamon, M.H. and Stecker, F.W. 1998, ApJ 493, 547
- Sigl, G. 1996, Space Sci. Rev. 75, 375
- Skopic, D.M., Asai, J., & Murphy, J.J., 1980, Phys. Rev. C21, 1746.
- Stanev, T., P.L. Biermann & J. Lloyd-Evans 1995, Phys. Rev. Letters 75, 3056
- Stanev, T. & A. Franceschini 1998, ApJ 494, L59
- Stecker, F.W. 1968, Phys. Rev. Letters 21, 1016
- Stecker, F.W. 1969, Phys. Rev. 180, 1264
- Stecker, F.W. 1998, Phys. Rev. Letters 80, 1816
- Stecker, F.W. & O.C. de Jager 1993, ApJ 415, L71
- Stecker, F.W. & O.C. De Jager 1997, in *Proc. Kruger Natl. Park Intl. Workshop on TeV Gamma-Ray Astrophysics*, (Space Research Unit Potchefstroom U.) ed. O.C. de Jager, p. 39
- Stecker, F.W. & O.C. de Jager 1998, Astron. & Ap 334, L85
- Stecker, F.W., O.C. de Jager & M.H. Salamon 1992, ApJ 390, L49
- Takahara, F. 1990, Prog. Theor. Phys. (Japan) 83, 1071
- Takeda, M. *et al.* 1998, Phys. Rev. Letters 81, 1163.
- Zatsepin, G.T. & V.A. Kuz'min 1966, Zh. Experim. i Teor. Fiz. - Pis'ma Redakt. 4, 114

Table 1. Photodisintegration energy thresholds (in MeV) for one-nucleon, two-nucleon, and α emission for all isotopes in the decay chain of ^{56}Fe

Z	A	(γ, n)	(γ, p)	$(\gamma, 2n)$	(γ, np)	$(\gamma, 2p)$	(γ, α)
26	56	11.2	10.2	20.5	20.4	18.3	7.6
26	54	13.4	8.9	24.1	20.9	15.4	8.4
25	55	10.2	8.1	19.2	17.8	20.4	7.9
24	54	9.7	12.4	17.7	20.9	22.0	7.9
24	53	7.9	11.1	20.0	18.4	20.1	9.1
24	52	12.0	10.5	21.3	21.6	18.6	9.4
24	50	13.0	9.6	23.6	21.1	16.3	8.6
23	51	11.1	8.1	20.4	19.0	20.2	10.3
23	50	9.3	7.9	20.9	16.1	19.3	9.9
22	50	10.9	12.2	19.1	22.3	21.8	10.7
22	49	8.1	11.4	19.8	19.6	20.8	10.2
22	48	11.6	11.4	20.5	22.1	19.9	9.4
22	47	8.9	10.5	22.1	19.2	18.7	9.0
22	46	13.2	10.3	22.7	21.7	17.2	8.0
21	45	11.3	6.9	21.0	18.0	19.1	7.9
20	48	9.9	15.8	17.2	24.2	29.1	14.4
20	46	10.4	13.8	17.8	22.7	22.7	11.1
20	44	11.1	12.2	19.1	21.8	21.6	8.8
20	43	7.9	10.7	19.4	18.2	19.9	7.6
20	42	11.5	10.3	19.8	20.4	18.1	6.2
20	40	15.6	8.3	29.0	21.4	14.7	7.0
19	41	10.1	7.8	17.9	17.7	20.3	6.2
19	40	7.8	7.6	20.9	14.2	18.3	6.4
19	39	13.1	6.4	25.2	18.2	16.6	7.2
18	40	9.9	12.5	16.5	20.6	22.8	6.8
18	38	11.8	10.2	20.6	20.6	18.6	7.2
18	36	15.3	8.5	28.0	21.2	14.9	6.6
17	37	10.3	8.4	18.9	18.3	21.4	7.8
17	35	12.6	6.4	24.2	17.8	17.3	7.0
16	36	9.9	13.0	16.9	21.5	25.0	9.0
16	34	11.4	10.9	20.1	21.0	20.4	7.9
16	33	8.6	9.6	23.7	17.5	18.2	7.1
16	32	15.0	8.9	28.1	21.2	16.2	6.9
15	31	12.3	7.3	23.6	17.9	20.8	9.7

Table 1—Continued

Z	A	(γ, n)	(γ, p)	$(\gamma, 2n)$	(γ, np)	$(\gamma, 2p)$	(γ, α)
14	30	10.6	13.5	19.1	22.9	24.0	10.6
14	29	8.5	12.3	25.7	20.1	21.9	11.1
14	28	17.2	11.6	30.5	24.6	19.9	10.0
13	27	13.1	8.3	24.4	19.4	22.4	10.1
12	26	11.1	14.1	18.4	23.2	24.8	10.6
12	25	7.3	12.1	23.9	19.0	22.6	9.9
12	24	16.5	11.7	29.7	24.1	20.5	9.2
11	23	12.4	8.8	23.5	19.2	24.1	10.5
10	22	10.4	15.3	17.1	23.4	26.4	9.7
10	21	6.8	13.0	23.6	19.6	23.6	7.3
10	20	16.9	12.8	28.5	23.3	20.8	4.7
9	19	10.4	8.0	19.6	16.0	23.9	4.0
8	18	8.0	15.9	12.2	21.8	29.1	6.2
8	17	4.1	13.8	19.8	16.3	25.3	6.4
8	16	15.7	12.1	28.9	23.0	22.3	7.2
7	15	10.8	10.2	21.4	18.4	31.0	11.0
7	14	10.6	7.6	30.6	12.5	25.1	11.6
6	13	4.9	17.5	23.7	20.9	31.6	10.6
6	12	18.7	16.0	31.8	27.4	27.2	7.4
5	11	11.5	11.2	19.9	18.0	30.9	8.7
5	10	8.4	6.6	27.0	8.3	23.5	4.5
4	9	1.7	16.9	20.6	18.9	29.3	2.5
3	7	7.3	10.0	12.9	11.8	33.5	2.5
3	6	5.7	4.6	27.2	3.7	26.4	1.5
2	4	20.6	19.8	28.3	26.1
2	3	7.7	5.5
1	2	2.2